Supplementary Information

Uptake and Release of Gaseous Species Accompanying the Reactions of Isoprene Photo-Oxidation Products with Sulfate Particles

by

Yingjun Liu (1), Mikinori Kuwata† (1), Karena A. McKinney* (1), and S.T. Martin* (1,2)

(1) School of Engineering and Applied Sciences, Harvard University, Cambridge, Massachusetts, USA

(2) Department of Earth and Planetary Sciences, Harvard University, Cambridge, Massachusetts, USA

E-mail: scot_martin@harvard.edu, kamckinney@seas.harvard.edu

Submitted: October 16, 2015

Physical Chemistry Chemical Physics

*To Whom Correspondence Should be Addressed

†Now at Asian School of the Environment, Nanyang Technological University, Singapore, and Earth Observatory of Singapore

Determination of uptake coefficient of IEPOX

The intensity decrease of $C_5H_6O^+$ ions upon injection of sulfate particles in this study can be used to estimate the reactive uptake coefficient γ of IEPOX isomers. The reactive uptake coefficient γ of species A is obtained as follows:[1]

$$\gamma = \frac{4RV}{w[A]'S} \tag{1}$$

where $[A]'$ is the steady-state concentration in the Reactor 2 with particle injection (molec m^{-3}), R is the uptake rate of species A (molec m^{-3} s^{-1}), S is the particle surface area (m^2), V is the reactor volume (m^3), and w is the mean molecular speed of M (m s^{-1}). R in Reactor 2 at steady state can be determined based on mass balance:

$$R = \frac{[A]'}{\tau} - \frac{[A]}{\tau} = \frac{\Delta[A]}{\tau} \tag{2}$$

where $[A]$ is the steady-state concentration in Reactor 2 without particle injection, $\Delta[A]$ is the concentration difference in the absence and presence of particles, and τ is the residence time in Reactor 2. Combing Equations (1) and (2), we have

$$\gamma = \frac{4V}{wS\tau}\frac{\Delta[A]}{[A]'} = \frac{4V}{wS\tau}\frac{\Delta I}{I'} \tag{3}$$

where I' is the signal intensity of one characteristic ion of species A measured by SRI-NO^+-TOF-MS in Reactor 2 with particle injection and ΔI is the intensity difference compared to that in the absence of particles. For a system of multiple components, Equation (3) is valid under the condition that I and ΔI can be dominantly attributed to species A.

To determine γ using Equation (3) for the current experimental conditions, the largest uncertainty lies in quantification of the reactive surface area S. Additional experiments show that diameter growth of the particle population in Reactor 2 ceases when the injection of sulfate particles is stopped (Fig. S3). The implication is that reactions go to completion for the majority of particles within the residence time in Reactor 2, possibility due to proton consumption by organosulfate formation. Decrease of acidity with reaction time for SOM formation from α-pinene ozonolysis on acidic sulfate particles is previously reported.[2] Due to the completion of the reaction for the majority of particles, the total reactive surface area is expected to be less than 50% of the measured particle surface area corrected for wall loss.[3] Given that only the upper limit of reactive surface area can be estimated, the estimated reactive uptake coefficient γ is a lower limit.

The method of estimating the reactive uptake coefficient used here is applicable only for ions which can be dominantly attributed to a single compound, such as the $C_5H_6O^+$ ion for IEPOX.[3] The estimated lower limit of uptake coefficients γ_{IEPOX} ranges from 0.08 to 0.20 for the investigated conditions (Fig S2a). These estimates are for initial uptake. For ions other than $C_5H_6O^+$, multiple compounds can contribute to the same ion.

As a further note, the particle populations of low and intermediate neutralization have different mode diameters (40 and 120 nm, respectively) as a result of the different methods of production. Kinetic effects, however, which can depend on particle size, do not appear to explain the observed dependence of uptake or release of compounds on the extent of particle neutralization because the reactions appear to have gone to completion (Fig. S3). Even so, the results reported herein might have some dependence on particle size depending on the underlying detailed mechanisms of gas-particle exchange of each reaction.

References

1. A. R. Ravishankara, *Science*, 1997, **276**, 1058-1065.
2. M. Jang, G. Cao and J. Paul, *Aerosol Sci Tech*, 2008, **42**, 409-420.
3. Y. J. Liu, M. Kuwata, B. F. Strick, F. M. Geiger, R. J. Thomson, K. A. McKinney and S. T. Martin, *Environ. Sci. Technol.*, 2015, **49**, 250-258.
4. D. Smith and P. Spanel, *Mass. Spectrom. Rev.*, 2005, **24**, 661-700.

Table S1. List of ions following each of the six types of *X*-dependence. An example of each type is shown in Figs. 3 and 4. Molecular assignments of the precursor compounds of all individual ions are not possible with the collected data sets alone, in part because authentic standards are not readily available. In addition, SRI-TOF-MS analysis can fragment large oxygenated molecules and also has limited capability to distinguish among isomeric species.[4]

X-dependence	Ions
N	$C_3H_7^+$ (*m/z* 43.054), $C_5H_8^+$ (*m/z* 68.062), $C_5H_7O^+$ (*m/z* 83.049), $C_3H_4NO_3^+$ (*m/z* 102.019), $C_4H_6NO_4^+$ (*m/z* 132.029)
L_{low}	$C_4H_5O^+$ (*m/z* 69.034), $C_4H_6O^+$ (*m/z* 70.041), $C_4H_7O^+$ (*m/z* 71.049), $C_4H_6NO_2^+$ (*m/z* 100.039), $C_4H_6NO_3^+$ (*m/z* 116.034), $C_5H_6NO_3^+$ (*m/z* 128.034), $C_4H_4NO_4^+$ (*m/z* 130.013)
L	$C_4H_7^+$ (*m/z* 55.054), $C_3H_5O^+$ (*m/z* 57.034), $C_5H_6O^+$ (*m/z* 82.041), $C_4H_5O_2^+$ (*m/z* 85.028), $C_5H_9O^+$ (*m/z* 85.065), $C_4H_6O_2^+$ (*m/z* 86.036), $C_4H_7O_2^+$ (*m/z* 87.044), $C_4H_8O_2^+$ (*m/z* 88.052), $C_5H_5O_2^+$ (*m/z* 97.028), $C_5H_6O_2^+$ (*m/z* 98.036), $C_5H_7O_2^+$ (*m/z* 99.044), $C_5H_8NO_3^+$ (*m/z* 130.050), $C_4H_8NO_4^+$ (*m/z* 134.045), $C_5H_6NO_4^+$ (*m/z* 144.029),
P_{low}	$C_3H_6NO_3^+$ (*m/z* 104.034), $C_5H_4NO_4^+$ (*m/z* 142.013), $C_6H_8NO_5^+$ (*m/z* 174.040), $C_5H_8NO_5^+$ (*m/z* 162.040), $C_6H_{10}NO_5^+$ (*m/z* 176.055), $C_6H_8NO_6^+$ (*m/z* 190.035), $C_7H_{12}NO_5^+$ (*m/z* 190.071)
P	$CH_2NO_3^+$ (*m/z* 76.003), $C_3H_6NO_2^+$ (*m/z* 88.039), $C_2H_4NO_3^+$ (*m/z* 90.019), $C_3H_4NO_4^+$ (*m/z* 118.013), $C_5H_8NO_4^+$ (*m/z* 146.045), $C_5H_6NO_5^+$ (*m/z* 160.024)
LP	$C_2H_3O^+$ (*m/z* 43.018), $C_5H_9O_2^+$ (*m/z* 101.060), $C_5H_7O_3^+$ (*m/z* 115.039), $C_5H_9O_3^+$ (*m/z* 117.055)

Table S2. Signal change Δ*I* of ions of Families L_{low}, *L*, P_{low}, *P*, and *LP* at $X = 0.02$ and of Families *L*, *P*, and *LP* at $X = 0.4$ (Fig. 5).

Family	Δ*I* (ncps)	Family	Δ*I* (ncps)		Family	Δ*I* (ncps)	Family	Δ*I* (ncps)		Family	Δ*I* (ncps)	
L_{low}	$X = 0.02$	*L*	$X = 0.39$	$X = 0.02$	P_{low}	$X = 0.02$	*P*	$X = 0.39$	$X = 0.02$	*LP*	$X = 0.39$	$X = 0.02$
$C_4H_6NO_2^+$	-84 ± 6	$C_5H_6O^+$	-76 ± 3	-111 ± 2	$C_3H_6NO_3^+$	104 ± 5	$C_5H_8NO_4^+$	16 ± 3	129 ± 6	$C_5H_9O_2^+$	-5.9 ± 1.1	-5.9 ± 1.2
$C_4H_5O^+$	-21 ± 2	$C_5H_7O_2^+$	-9.1 ± 1.2	-27 ± 1	$C_6H_8NO_5^+$	8.4 ± 1.0	$C_3H_6NO_2^+$	3.6 ± 0.9	22 ± 1	$C_2H_3O^+$	-5.6 ± 2.1	0.2 ± 1.8
$C_5H_6NO_3^+$	-9.4 ± 0.8	$C_5H_8NO_3^+$	-6.4 ± 1.4	-12 ± 1.6	$C_5H_8NO_5^+$	5.4 ± 0.7	$C_2H_4NO_3^+$	2.7 ± 2.0	17 ± 2	$C_5H_9O_3^+$	-1.2 ± 0.5	4.0 ± 0.7
$C_4H_6NO_3^+$	-6.9 ± 1.4	$C_4H_8NO_4^+$	-5.1 ± 0.8	-12 ± 0.9	$C_7H_{12}NO_5^+$	3.7 ± 0.3	$C_5H_6NO_5^+$	2.5 ± 0.6	4.9 ± 0.6	$C_5H_7O_3^+$	-0.7 ± 0.6	-0.4 ± 0.5
$C_4H_7O^+$	-4.4 ± 1.0	$C_4H_5O_2^+$	-4.7 ± 0.7	-9.9 ± 0.7	$C_6H_{10}NO_5^+$	1.4 ± 0.5	$C_3H_4NO_4^+$	1.1 ± 0.6	4.2 ± 0.9			
$C_4H_4NO_4^+$	-2.6 ± 0.6	$C_4H_7^+$	-3.8 ± 1.0	-12 ± 0.1	$C_5H_4NO_4^+$	1.3 ± 0.3	$CH_2NO_3^+$	0.5 ± 0.5	1.9 ± 0.5			
$C_4H_6O^+$	-1.5 ± 0.8	$C_5H_9O^+$	-1.9 ± 0.4	-4.3 ± 0.4	$C_6H_8NO_6^+$	0.7 ± 0.2						
		$C_4H_6O_2^+$	-1.8 ± 0.6	-3.5 ± 0.5								
		$C_5H_6NO_4^+$	-1.7 ± 0.6	-2.2 ± 0.7								
		$C_3H_5O^+$	-1.6 ± 1.0	-2.1 ± 1.1								
		$C_5H_5O_2^+$	-1.2 ± 0.3	-4.8 ± 0.3								
		$C_4H_7O_2^+$	-1.0 ± 0.4	-2.4 ± 0.5								
		$C_4H_8O_2^+$	-0.6 ± 0.6	-1.7 ± 0.7								
		$C_5H_6O_2^+$	-0.6 ± 0.4	-2.0 ± 0.4								
Sum	-130 ± 7		-116 ± 4	-207 ± 4		125 ± 5		27 ± 4	179 ± 6		-13 ± 2	-2.0 ± 2.3

Table S3. Summed molecular uptake and release estimated from signal change Δ*I* of individual ions (Table S2) assuming ± 50% uncertainty in the conversion to species concentrations.

	X = 0.39	*X* = 0.02
Summed molecular uptake (ppb)	-5.9 ± 1.8	-16 ± 3
Summed molecular release (ppb)	1.2 ± 0.4	14 ± 4
Release / uptake (%)	21 ± 9	90 ± 30

List of Figures

Figure S1. Dependence of signal intensity I' on the extent X of neutralization in presence of particles for three ions in each of families (a) L_{low}, (b) L, (c) P_{low}, and (d) P. The shaded areas represent confidential intervals of 99.7% of signal intensity I in the absence of sulfate particles. For many values of X, the signal intensity does not change in the presence of particles (i.e., data points overlying the shaded areas).

Figure S2. Dependence of (a) lower-limit of uptake coefficient γ_{IEPOX} of IEPOX, (b) intensities $C_2H_3O^+$ ion, and (c) mass concentration M_{SOM} of SOM on the extent X of neutralization of particles.

Figure S3. Evolution of particle number-diameter distribution following termination of sulfate particle injection in the second reactor. SOM is produced by reactive uptake of isoprene oxidation products by acidic sulfate particles. Injection of isoprene oxidation products continues after termination of particle injection.

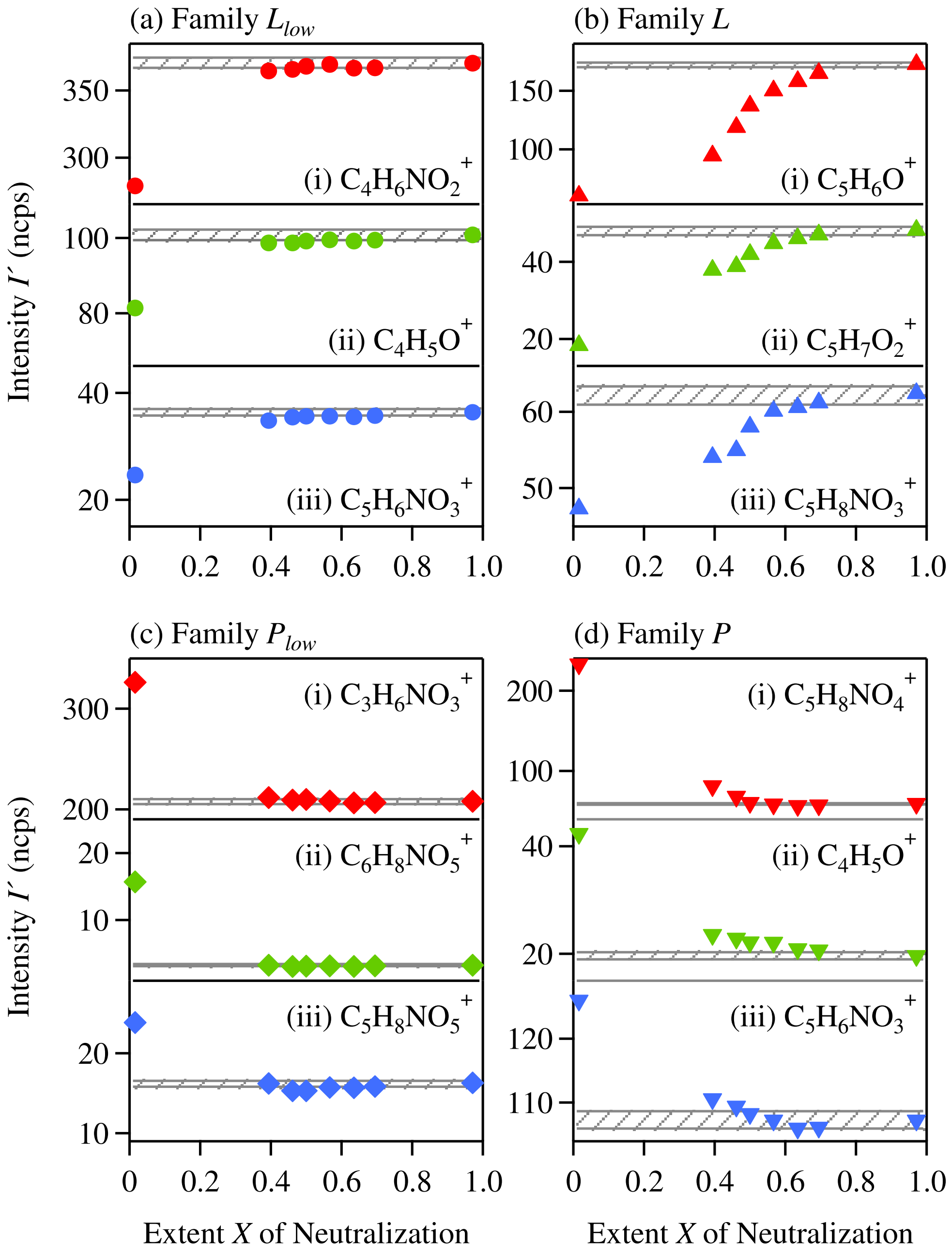
(a) Family L_{low}
(b) Family L
(c) Family P_{low}
(d) Family P
(i) $C_4H_6NO_2^+$
(ii) $C_4H_5O^+$
(iii) $C_5H_6NO_3^+$
(i) $C_5H_6O^+$
(ii) $C_5H_7O_2^+$
(iii) $C_5H_8NO_3^+$
(i) $C_3H_6NO_3^+$
(ii) $C_6H_8NO_5^+$
(iii) $C_5H_8NO_5^+$
(i) $C_5H_8NO_4^+$
(ii) $C_4H_5O^+$
(iii) $C_5H_6NO_3^+$
Intensity I′ (ncps)
Extent X of Neutralization
350
300
100
80
40
20
150
100
40
20
60
50
300
200
20
10
20
10
200
100
40
20
120
110
0
0.2
0.4
0.6
0.8
1.0

Figure S1

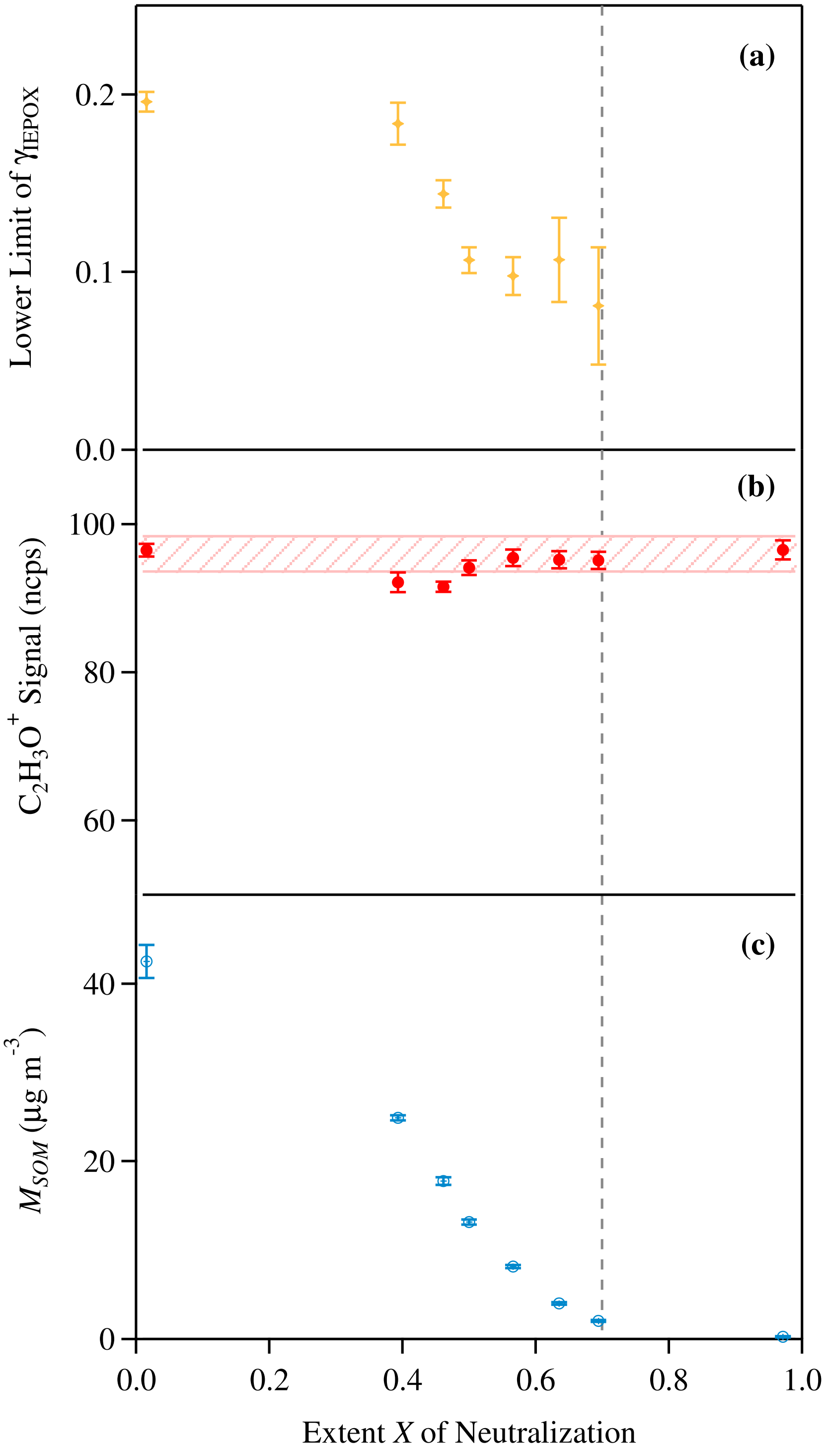
(a)
(b)
(c)
Lower Limit of γ_{IEPOX}
0.0
0.1
0.2
$C_2H_3O^+$ Signal (ncps)
60
80
100
M_{SOM} (µg m^{-3})
0
20
40
0.0
0.2
0.4
0.6
0.8
1.0
Extent X of Neutralization

Figure S2

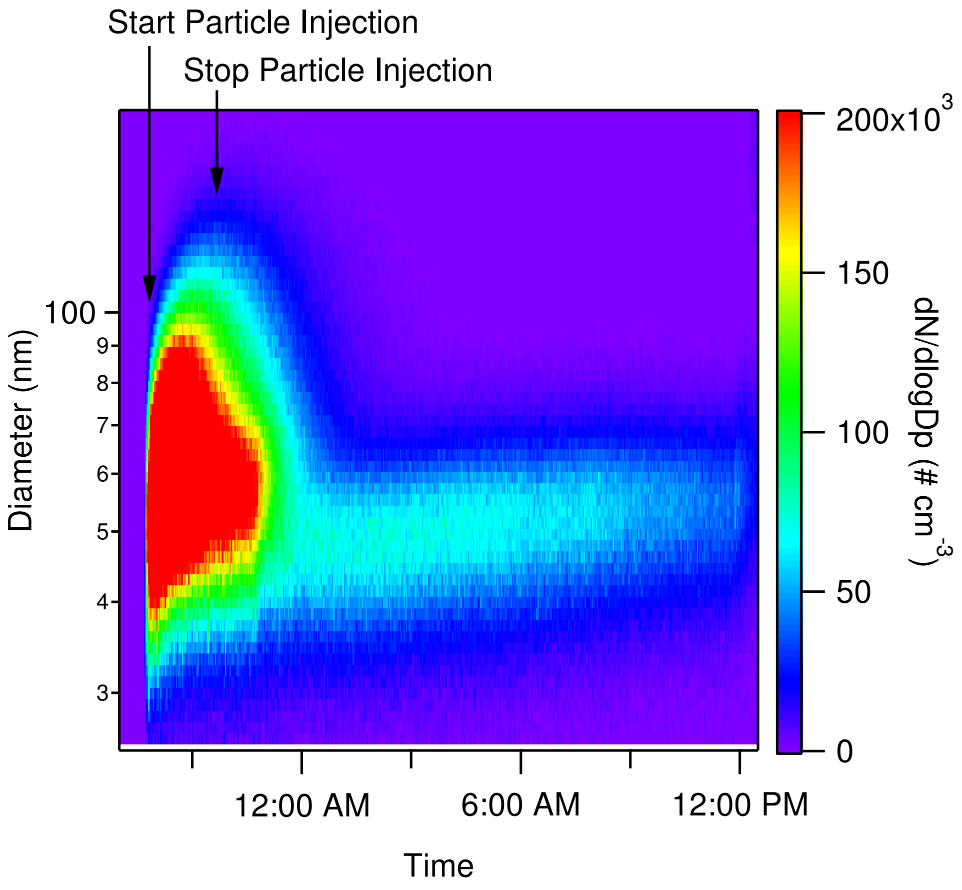
Start Particle Injection
Stop Particle Injection
Diameter (nm)
100
9
8
7
6
5
4
3
12:00 AM
6:00 AM
12:00 PM
Time
200x10^3
150
100
50
0
dN/dlogDp (# cm^-3)

Figure S3